



University of Warwick institutional repository: <http://go.warwick.ac.uk/wrap>

This paper is made available online in accordance with publisher policies. Please scroll down to view the document itself. Please refer to the repository record for this item and our policy information available from the repository home page for further information.

To see the final version of this paper please visit the publisher's website. Access to the published version may require a subscription.

Author(s): W. J. Lewis

Article Title: A Mathematical Model for Assessment of Material Requirements for Cable Supported Bridges: Implications for Conceptual Design

Year of publication: 2012 (Forthcoming)

Link to published article:

<http://www.sciencedirect.com/science/journal/01410296>

Publisher statement: None

***A Mathematical Model for Assessment of Material Requirements for Cable Supported Bridges:
Implications for Conceptual Design.***

W. J. Lewis, Inz, MSc, PhD, CEng, FICE
School of Engineering, University of Warwick
Coventry CV4 7AL, UK
Tel: +44 24 76 523 138
Email: W. J. Lewis@warwick.ac.uk

Abstract

Recent technological developments have led to improvements in the strengths of materials, such as the steel and wire ropes used in the construction of cable supported bridges. This, combined with technological advancements in construction, has encouraged the design of structures with increasing spans, leaving the question of material and environmental costs behind. This paper presents a refined mathematical model for the assessment of relative material costs of the supporting structures for cable-stayed and cable suspension bridges. The proposed model is more accurate than the ones published to date in that it includes the self weight of the cables and the pylons. Comparisons of material requirements for each type of bridge are carried out across a range of span/dip ratios. The basis of comparison is the assumption that each structure is made of the same material (steel) and carries an identical design load, q , exerted by the deck. Calculations are confined to a centre span of a three-span bridge, with the size of the span ranging from 500 m to 3000 m. Results show that the optimum span/dip ratio, which minimises material usage, is 3 for a cable-stayed (harp type) bridge, and 5 for a suspension structure. The inclusion of the self weight of cable in the analysis imposes limits on either the span, or span/dip ratio. This effect is quantified and discussed with reference to the longest cable-supported bridges in the world completed to date and planned in the future.

Keywords: suspension bridges; cable-stayed bridge; material costs; span/dip ratio

1. Background

Over the years, a number of studies related to the assessment of the volume of material and material costs in cable-stayed and suspension bridges have been produced. A relatively simple model used by French¹, which excluded the self weight of cables and pylons, demonstrated that, with the cost of the cable material twice that of the pylons, the optimum span/dip ratio for the suspension bridges was 9:1. This prediction was based on the allowable stresses in the cables of 600N/mm^2 , and 120N/mm^2 in the pylons, which values were significantly lower than the up-to-date strengths of 700N/mm^2 and 160N/mm^2 , respectively, as used by Gimsing² and the author of this paper.

The model proposed by Gimsing², included the self weight of pylons, as this was viewed as important in the final assessment of the 'lightness' of the structure, but excluded the self weight of the cables. Surprisingly, it also excluded the additional weight of the deck required in the cable-stayed bridge to resist the substantial membrane forces that develop there. Based on these assumptions, the model predicted an optimum span/dip ratio for both suspension and cable-stayed (fan type) bridges with the main span of 500 m to be ~ 6.6 . This was based on material costs, assuming that the unit cost of steel in the pylons was the same for both systems, but the ratios of the unit price of cable to pylon were different: 1.75 in the case of the suspension bridge, and 2.5 for the cable-stayed structure. This optimum span/dip ratio was unchanged for the suspension bridge when the main span was doubled, i.e., equal to 1000 m.

Earlier work by Podolny and Scalzi³ stated that the most economical span/dip ratio for the cable-stayed bridges was 5:1, and 8:1 for the suspension type. It reported on the work of Leonhardt⁴, which produced a modification factor on the material volume used by the cable when the cable weight was included. Taking the span/dip ratio of 9:1 for the suspension bridge, a 5:1 for the cable-stayed one, and a central span of 3280 ft (1000 m), the proposed modification increased the cable steel requirements for the suspension bridge by 17%, but only by 5% for the cable-stayed structure.

The work quoted above highlights the issue of scale. Parsons⁵ showed that on the basis of an approximate relationship between the cost per unit area of roadway and the span, suspension bridges were more economic for spans above 600m (the height of the pylons was not given). He stressed the fact that the span of a suspension bridge was limited only by the tensile strength of the cable and this prime structural element is inherently stable, while the span of a cable-stayed structure is limited by the compressive strength of the deck which is inherently unstable.

More recently, Croll⁶ offered a simple analysis of the relative usage of the material by cable-stayed (harp type) and suspension bridges, respectively. In common with Gimsing² and French¹, the

calculation for the volume of the material was based on the design principle that the cross section of any load-carrying member should not be stressed beyond an assumed value of working stress. The analysis ignored the self weight of the cables and the pylons. Surprisingly, in the initial model, no distinction was made between the tensile strength of the cables and the pylons, and simply one value was used for both. The modification of the model, following contributions from H.C. Dalton⁷ and M. J. French⁷, included not only material usage, but also material cost. The calculated material volumes were factored using a compound material and cost parameter, β , expressed as a ratio of tensile to compressive stresses, further multiplied by a ratio of unit costs of cable to pylon. The factor β ranged between 1 and 5. After this modification, the results showed the suspension bridges to be more cost efficient than the cable-stayed ones, for span/dip ratio greater than 4. They also showed an optimum span/dip ratio for a cable-stayed bridge to be between 2 and 3 and, for a suspension structure, between 4 and 7 (depending on the β factor).

In view of the inconsistent and conflicting information produced to date, a more rigorous analysis of material usage (including material cost) is needed in the design of cable supported bridges. This paper addresses this problem by examining the subject more closely and presenting an analysis that is as close to reality as possible.

2. Suspension bridge

2.1. General

Figure 1 shows the basic geometry of a suspension cable bridge in which L is the centre span of the bridge and h is the height of towers above the deck. The distribution of forces in the main structural elements is shown in Fig.1 (a).

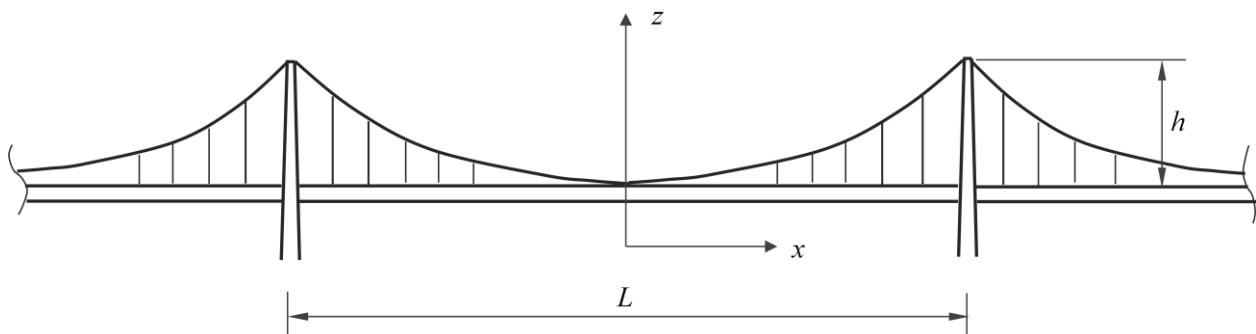


Fig .1. Basic geometry of a suspension cable bridge

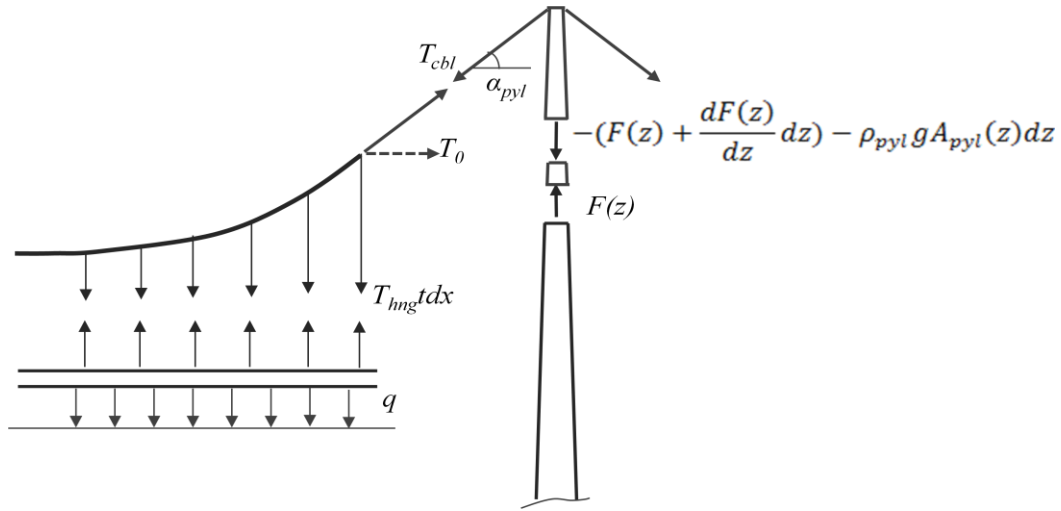


Fig. 1(a). Diagrammatic representation of forces in the main structural elements of the bridge

The prediction of material usage is based on the centre span. The general assumptions are as follows:

- (i) the bridge is subjected to a uniformly distributed design deck load, q , the weight of the cables and the pylons;
- (ii) the shape adopted by the suspension cables is assumed to be a parabola. This shape corresponds to the case of a uniformly distributed load from the deck, q , and follows the usual assumption that hanger and cable weights are negligible compared to q ;
- (iii) the hangers form a uniform 'curtain' suspended from the cables and stressed by q . It is shown later that the stress due to the self weight of hangers is negligible. Hence, the amount of material used by them is simply proportional to the area under the parabolic cable;
- (iv) the cross section of the suspension cable is calculated by dividing the maximum tension force in the cable by an assumed constant value of working (tensile) stress, σ_t ; the product of the cross section area and the length of the cable gives the volume of the material required;
- (iv) each pylon is assumed to carry a half of the deck weight, $qL/2$, the self weight of the cables and their own weight; their cross section area varies with height in such a manner as to ensure constant stress.

2.2. Calculation of the volume of material used by hangers

The hangers, modelled as a 'curtain' of individual strands, have thickness, t . If ρ_h is the density of the hanger and $T_{hng}(z)$ is the tensile stress, the equation of vertical equilibrium of the hanger element, $tdxdz$, (Fig. 1(a)) is

$$-T_{hng}tdx + \left(T_{hng}tdx + \frac{d}{dz}(T_{hng}tdx)dz\right) - \rho_h gtdxdz = 0, \quad (2.2.1)$$

which gives $\frac{dT_{hng}(z)}{dz} = \rho_h g$, or

$$T_{hng}(z) = \rho_h gz + C \quad (2.2.2)$$

At the deck level,

$$T_{hng}(0)tdx - qdx = 0, \quad T_{hng}(0) = \frac{q}{t}$$

and hence

$$T_{hng}(z) = \rho_h gz + \frac{q}{t} \quad (2.2.3)$$

The thickness of the curtain is sized on the basis of the maximum stress, which occurs at $z = h$. With the assume maximum working stress, σ_t ,

$$\sigma_t = \rho_h gz + \frac{q}{t},$$

the thickness of the ‘curtain’ is

$$t = \frac{q}{\sigma_t - \rho_h gh}, \quad (2.2.4)$$

where g is the gravitational constant.

Denoting the area of the ‘curtain’ below the suspension cable by A_{curt} , the total volume of the material used by the hangers, $V_{hng, susp}$ is

$$V_{hng, susp} = A_{curt}t = \frac{1}{3}hLt = \frac{qhL}{\sigma_t - \rho_h gh} \times \frac{1}{3} = \frac{qhL}{\sigma_t} \left(\frac{1}{3} \times \frac{1}{1 - \frac{\rho_h gh}{\sigma_t}} \right). \quad (2.2.5)$$

Introducing the span/h ratio, $r=L/h$, and noting the term $\frac{\rho_h gh}{\sigma_t}$ to be small, the above equation becomes

$$V_{hng, susp} = \frac{qhL}{\sigma_t} \times \frac{1}{3} = \frac{qL^2}{\sigma_t} \frac{1}{r} \times \frac{1}{3} \quad (2.2.6)$$

2.3 Volume of material used by the suspension cable

The cable follows a parabolic shape and has a constant cross section A_{cbl} . It carries the weight of the deck and its own weight. Therefore, for a symmetric structure, the volume of cable material, $V_{cbl, susp}$, is

$$V_{cbl, susp} = 2A_{cbl}L_{cbl}, \quad (2.3.1)$$

where L_{cbl} is the length of the cable measured from centre span ($L_{cbl}=L/2$). For a parabola,

$z = h\left(\frac{2x}{L}\right)^2$, the slope is $\frac{dz}{dx} = \frac{8hx}{L^2} = \tan \alpha$, and hence

$$L_{cbl} = \int_0^{L/2} \sqrt{1 + \left(\frac{8hx}{L^2}\right)^2} dx = \frac{L^2}{8h} \left\{ \frac{1}{2} \ln[a + \sqrt{b}] + \frac{a}{2} \sqrt{b} \right\}, \quad (2.3.2)$$

where $a = \frac{4h}{L}$, and $b = 1 + \left(\frac{4h}{L}\right)^2$.

The cross section area of cable, A_{cbl} , is given by

$$A_{cbl} = T_{cbl}^{\max} / \sigma_t, \quad (2.3.3)$$

where T_{cbl}^{\max} is the maximum tension force in the cable at the pylon attachment, given by

$$T_{cbl}^{\max} = \frac{T_0}{\cos \alpha_{pyl}} = T_0 \sqrt{1 + \tan^2 \alpha_{pyl}}, \quad (2.3.4)$$

and T_0 is the horizontal component of the cable force, known to be constant.

Since the slope of the curve is $\frac{dz}{dx} = \frac{8hx}{L^2} = \tan \alpha$, then at the pylon attachment (at $x = L/2$),

$\frac{dz}{dx} = \tan \alpha_{pyl} = \frac{4h}{L} = a$, and $1 + \tan^2 \alpha_{pyl} = b$.

Hence, eqn.(2.3.4) becomes $T_{cbl}^{\max} = T_0 \sqrt{b}$

and the vertical load on the pylon, $T_0 \tan \alpha_{pyl} = T_0 a$, due to the weight of the semi-span and self weight of the cables, is

$$T_0 a = \frac{qL}{2} + \{L_{cbl} A_{cbl}\} \rho_{cbl} g = \frac{qL}{2} + \left\{ \frac{L_{cbl} T_0}{\sigma_t} \sqrt{1 + \left(\frac{4h}{L}\right)^2} \right\} \rho_{cbl} g, \quad (2.3.5)$$

where ρ_{cbl} is the density of the cable, and g the gravitational constant.

Thus,

$$T_0 = \frac{qL}{2 \left[a - \rho_{cbl} g \left(\frac{L_{cbl}}{\sigma_t} \sqrt{b} \right) \right]} = qLT_0^{non-dim} \quad (2.3.6)$$

where $T_0^{non-dim}$ is a non-dimensional term in eqn (2.3.6).

Consequently, the required cross section of cable is (eqns.2.3.3 and 2.3.4),

$$A_{cbl} = \frac{T_0 \sqrt{b}}{\sigma_t} \quad (2.3.7)$$

and the volume of the material used by the cable is

$$\begin{aligned} V_{cbl,susp} &= 2A_{cbl}L_{cbl} = \frac{qLh}{\sigma_t} \left\{ \frac{\sqrt{b}}{2 \left[a - \rho_{cbl} g \left(\frac{L_{cbl}}{\sigma_t} \sqrt{b} \right) \right]} \frac{L^2}{8h^2} (\ln[a + \sqrt{b}] + a\sqrt{b}) \right\} \\ &= \frac{qLh}{\sigma_t} V_{cbl,susp}^{non-dim} = \frac{qL^2}{\sigma_t} \frac{1}{r} \{ V_{cbl,susp}^{non-dim} \}, \end{aligned} \quad (2.3.8)$$

where $V_{cbl,susp}^{non-dim}$ is a non-dimensional constant in (2.3.8) for a given L/h ratio.

It can be seen from eqn (2.3.6) that in order to get sensible values for T_0 we must have

$$\left\{ a - \rho_{cbl} g \frac{L_{cbl}}{\sigma_t} \sqrt{b} \right\} > 0. \quad (2.3.9)$$

A further discussion of the above restriction is given in Section 4.

2.4 Volume of material used by the pylons

Each pylon carries a half of the total load applied by the deck, the self weight of cables from the centre span, and its own weight. The calculation for the volume of the material required by the pylons can be based on the assumption of constant stress, or a constant cross section along pylon's height. Pursuing the more rigorous approach based on the assumption of constant stress, leads to a set of calculations given below.

If ρ_{pyl} denotes the density of the pylon material, A_{pyl} the cross section area, and $F(z)$, a compression force at any cross section, then vertical equilibrium gives

$$F(z) - \left(F(z) + \frac{dF(z)}{dz} dz \right) - \rho_{pyl} g A_{pyl}(z) dz = 0 \quad (2.4.1)$$

Thus, the variation of the compressive force over the height of the pylon is (Fig. 1(a))

$$\frac{dF(z)}{dz} + \rho_{pyl} g A_{pyl}(z) = 0 , \quad (2.4.2)$$

Assuming a constant working stress, σ_c , in the pylon,

$$F(z) = \sigma_c A_{pyl}(z) \quad (2.4.3)$$

and

$$\frac{dA_{pyl}(z)}{dz} = -\frac{\rho_{pyl} g}{\sigma_c} A_{pyl}(z) = -\lambda A_{pyl}(z) , \quad (2.4.4)$$

where $\lambda = \frac{\rho_{pyl} g}{\sigma_c}$.

Separating the variables and integrating gives,

$$A_{pyl}(z) = C e^{-\lambda z} \quad (2.4.5)$$

where C is a constant, which can be found from the condition that at $z=h$,

$$A_{pyl}(z) = \frac{F_p}{\sigma_c} = C e^{-\lambda h} , \quad (2.4.6)$$

giving

$$C = \frac{F_p}{\sigma_c} e^{\lambda h} \quad (2.4.7)$$

where F_p is the maximum force applied to the top of the pylon by the weight of the decking and the cables, and is given by

$$F_p = T_0 \tan \alpha_{pyl} = T_0 \frac{4h}{L} . \quad (2.4.8)$$

The required cross section of pylon is now

$$A_{pyl}(z) = \left(\frac{F_p}{\sigma_c} e^{\lambda h} \right) e^{-\lambda z} = \frac{F_p}{\sigma_c} e^{\lambda(h-z)} , \quad (2.4.9)$$

which shows that the cross section area does not vary linearly.

The volume of the pylon material is, therefore

$$\begin{aligned} V_{pyl,susp} &= \int_0^h (A_{pyl}(z)) dz = \frac{F_p}{\sigma_c} \int_0^h e^{\lambda(h-z)} dz = -\frac{F_p}{\sigma_c \lambda} \left[e^{\lambda(h-z)} \right]_0^h \\ &= \frac{F_p}{\sigma_c \lambda} \left[e^{\lambda h} - 1 \right] \end{aligned} \quad (2.4.10)$$

Expanding $e^{\lambda h} - 1$ to third order, and substituting for F_p from (2.4.5) gives

$$V_{pyl,susp} = \frac{4T_0 h}{L \sigma_c} \left(h + \lambda h \frac{h}{2} + \lambda^2 h^2 \frac{h}{6} \right), \quad (2.4.11)$$

After substitution for T_0 from (2.3.6) and assuming $\sigma_c = \sigma_t / \gamma$ (in later comparisons, γ is taken as 700/160)

$$V_{pyl,susp} = \frac{qLh}{\sigma_t} \left\{ \gamma \frac{4T_0^{non-dim}}{L} \left(h + \lambda h \frac{h}{2} + \lambda^2 h^2 \frac{h}{6} \right) \right\} = \frac{qLh}{\sigma_t} V_{pyl,susp}^{non-dim} = \frac{qL^2}{\sigma_t} \frac{1}{r} \left\{ V_{pyl,susp}^{non-dim} \right\} \quad (2.4.12)$$

where $V_{pyl,susp}^{non-dim}$ is a non-dimensional term in (2.4.12). Thus, the total volume of material used by the supporting elements of a suspension bridge is

$$V_{susp}^{total} = V_{hng,susp} + V_{cbl,susp} + V_{pyl,susp} = \frac{qLh}{\sigma_t} \left\{ \frac{1}{3} + V_{cbl,susp}^{non-dim} + V_{pyl,susp}^{non-dim} \right\} \quad (2.4.13)$$

or

$$V_{susp}^{total} = \frac{qL^2}{\sigma_t} \frac{1}{r} \left\{ \frac{1}{3} + V_{cbl,susp}^{non-dim} + V_{pyl,susp}^{non-dim} \right\} \quad (2.4.14)$$

3. Cable stayed bridge

3.1 General

The assumptions made with respect to the cable stayed bridge shown in Figure 2 are similar to those made in respect of a suspension bridge. The basic approach to the calculation of material volume is the same, but the detailed calculations are somewhat different due to a difference in structural action of the bridge.

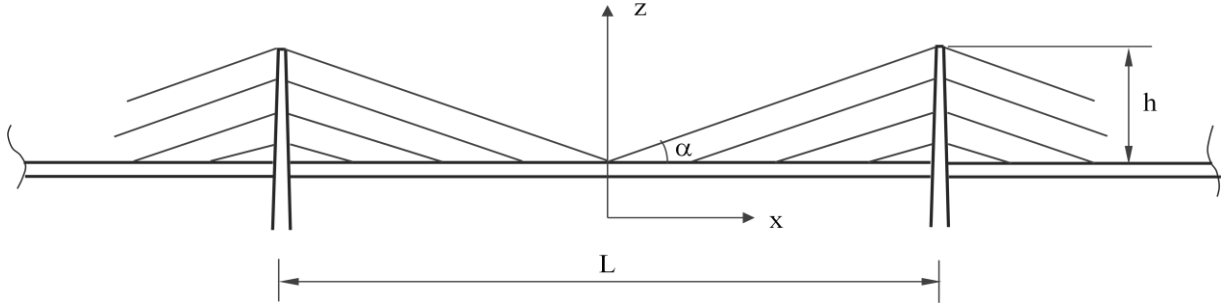


Fig. 2. Basic geometry of a cable-stayed bridge

The main assumptions and description of the model for the assessment of material requirements are as follows:

- (i) the bridge is subjected to a uniformly distributed deck load, q , and has to carry the weight of the cables and the pylons;
- (ii) the cables are represented by an equivalent ‘curtain’ of material. The thickness of the curtain is found as the ratio of the maximum tension to an assumed working (tensile) stress σ_t . The volume of the curtain is proportional to the area under the outermost cable;
- (iii) the bridge has to carry additional membrane forces transmitted by the cables to the deck. These are shown to vary from $+qL^2/8h$ to $-qL^2/8h$, (Section 3.3 and Figure 2(b)). With this arrangement, a horizontal force of $qL^2/8h$ will develop at the end supports, as in the case of the suspension bridge.
- (iv) pylons are assumed to carry a varying applied load over the height of the tower and have constant compressive stress.

3.2 Volume of material used by the cables

Assuming the cables are represented by a ‘curtain’ of constant thickness, the volume of the material for a half-span is given by

$$V_{cbl,stay} = \frac{1}{2} hLt, \quad (3.2.1)$$

where t is the thickness of the ‘curtain’, determined from the equilibrium equations that include cable weight.

It is assumed that the ‘curtain’ is composed of individual strands, in which the tension field varies along the length of each strand (Fig. 2(a)).

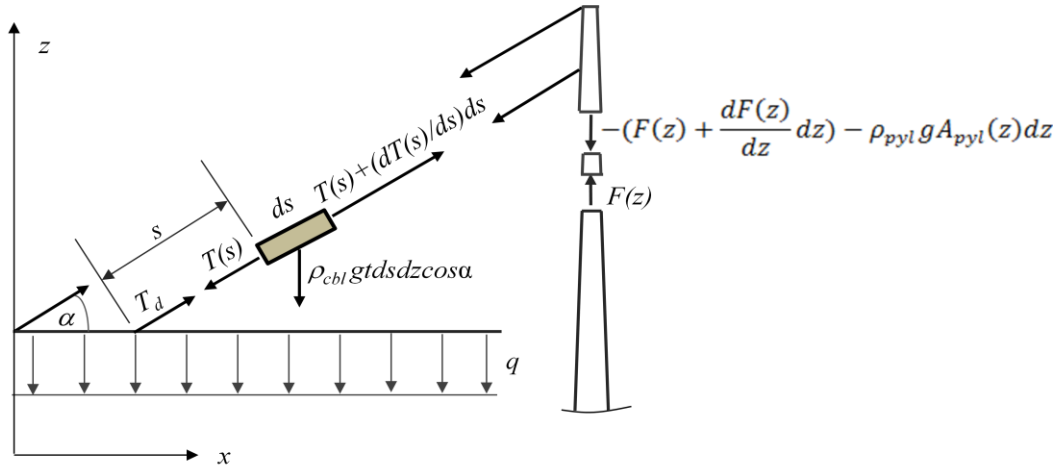


Fig. 2(a) Diagrammatic representation of forces in the main cable and the pylon

If $T(s)$ represent the force per unit width of the strand, then the vertical equilibrium of the strand element ds , which has a volume $t ds dz \cos \alpha$, mass density ρ_{cbl} , and width $dz \cos \alpha$, is given by

$$-T dz \cos \alpha \sin \alpha + \left[T dz \cos \alpha \sin \alpha + \frac{d(T dz \cos \alpha \sin \alpha)}{ds} ds \right] - \rho_{cbl} g t ds dz \cos \alpha = 0 \quad (3.2.2)$$

$$\text{or} \quad \sin \alpha \frac{dT(s)}{ds} - \rho_{cbl} g t = 0. \quad (3.2.3)$$

Integrating (3.2.3) with respect to s gives:

$$\sin \alpha T(s) - \rho_{cbl} g t s = C \quad (3.2.4)$$

where C is an arbitrary constant. When $s = 0$ (deck level), $C = \sin \alpha T(0)$

Vertical equilibrium at the deck level, gives

$$T(0) dz \cos \alpha \sin \alpha - q dx = 0$$

or

$$T(0) = \frac{q}{\cos \alpha \sin \alpha} \frac{dx}{dz} \quad (3.2.5)$$

where $dz = dx \tan \alpha$, and so

$$C = T(0) \sin \alpha = \frac{q \sin \alpha}{\cos \alpha \sin \alpha \tan \alpha} = \frac{q}{\sin \alpha} \quad (3.2.6)$$

Substituting (3.2.6) into (3.2.4) gives

$$\sin \alpha T(s) = \rho_{cbl} g t s + \frac{q}{\sin \alpha}$$

or

$$T(s) = \frac{1}{\sin \alpha} \left(\rho_{cbl} g t s + \frac{q}{\sin \alpha} \right)$$

The maximum value of tension, T_{\max} , corresponds to $s = h/\sin \alpha$ and thus

$$T_{\max} = \frac{1}{\sin \alpha} \left(\rho_{cbl} g t \frac{h}{\sin \alpha} + \frac{q}{\sin \alpha} \right) \quad (3.2.7)$$

At the deck level, the cable weight is zero and, therefore, the tension is

$$T_d = \frac{q}{\sin^2 \alpha} \quad (3.2.8)$$

The thickness of the curtain, t , is found by using $\sigma_t t = T_{\max}$, and hence

$$\sigma_t t = \frac{1}{\sin^2 \alpha} (\rho_{cbl} g t h + q)$$

from which

$$t = \frac{q}{\sigma_t \sin^2 \alpha - \rho_{cbl} g h} \quad (3.2.9)$$

where

$$\sin \alpha = \frac{2h}{\sqrt{4h^2 + L^2}}$$

It can be seen that the denominator in (3.2.9) can become zero, or negative. This indicates that, at certain spans and heights, the stress due to the weight of the cable may become equal to, or greater, than the allowable tensile stress, unless a restriction on the geometry of the bridge is imposed. This point is picked up in section 4, when discussing span restrictions.

Introducing a non-dimensional factor, $t^{non-dim}$, into (3.2.9) gives

$$t = \frac{q}{\sigma_t} t^{non-dim}, \quad (3.2.10)$$

in which

$$t^{non-dim} = \frac{1}{\sin^2 \alpha - \frac{\rho_{cbl} g h}{\sigma_t}}, \quad (3.2.11)$$

the volume of the material used by the cables is

$$V_{cbl,stay} = 2 \times \frac{1}{2} \frac{L}{2} h t = \frac{q h L}{\sigma_t} \left(\frac{1}{2} t^{non-dim} \right) = \frac{q L^2}{\sigma_t} \frac{1}{r} \left(\frac{1}{2} t^{non-dim} \right). \quad (3.2.12)$$

3.2.1 The case of varying cable thickness.

An alternative assessment of the cable usage can be made by assuming that t varies along the pylon (depending on the attachment point), but remains constant for each individual strand. In this case, the variable thickness, t_{var} is given by

$$t_{\text{var}} = \frac{q}{\sigma_t \sin^2 \alpha - \rho_{\text{cbl}} g z} \quad (3.2.13)$$

The volume of each strand, V_{strand} , is $lt_{\text{var}} dz \cos \alpha$, and with $l = z / \sin \alpha$

$$V_{\text{strand}} = \frac{t_{\text{var}} z dz}{\tan \alpha}$$

and, therefore, the volume of the curtain material using varying thickness is

$$V_{\text{cbl,stay}}^{\text{var}} = \int_0^h \frac{t_{\text{var}} z dz}{\tan \alpha} = \frac{q}{\tan \alpha} \int_0^h \frac{z dz}{\sigma_t \sin^2 \alpha - \rho_{\text{cbl}} g z} \quad (3.2.14)$$

The evaluation of the above integral gives the volume of cable material for 2 curtains, as

$$\begin{aligned} V_{\text{cbl,stay}}^{\text{var}} &= \frac{q h L}{\sigma_t} \left\{ \frac{\sigma_t^2}{(\rho_{\text{cbl}} g)^2 h^2 \left(1 + \frac{r^2}{4}\right)} \ln \frac{\sigma_t}{\sigma_t - \rho_{\text{cbl}} h \left(1 + \frac{r^2}{4}\right)} - \frac{\sigma_t}{\rho_{\text{cbl}} g h} \right\} \\ &= \frac{q L^2}{\sigma_t} \frac{1}{r} \left\{ \frac{\sigma_t^2}{(\rho_{\text{cbl}} g)^2 h^2 \left(1 + \frac{r^2}{4}\right)} \ln \frac{\sigma_t}{\sigma_t - \rho_{\text{cbl}} h \left(1 + \frac{r^2}{4}\right)} - \frac{\sigma_t}{\rho_{\text{cbl}} g h} \right\} \end{aligned} \quad (3.2.15)$$

Results obtained from the above equation showed a small reduction in the cable volume, compared to the case of the constant cross-section of cable curtain, given by eqn (3.2.11). For span $L=1000$ m, for example, the reduction is 4% and 6% for $r=3$ and $r=5$, respectively.

3.3. Additional volume of the material in the deck

The deck of the cable stayed bridge develops membrane forces, which can be determined using energy theorems.

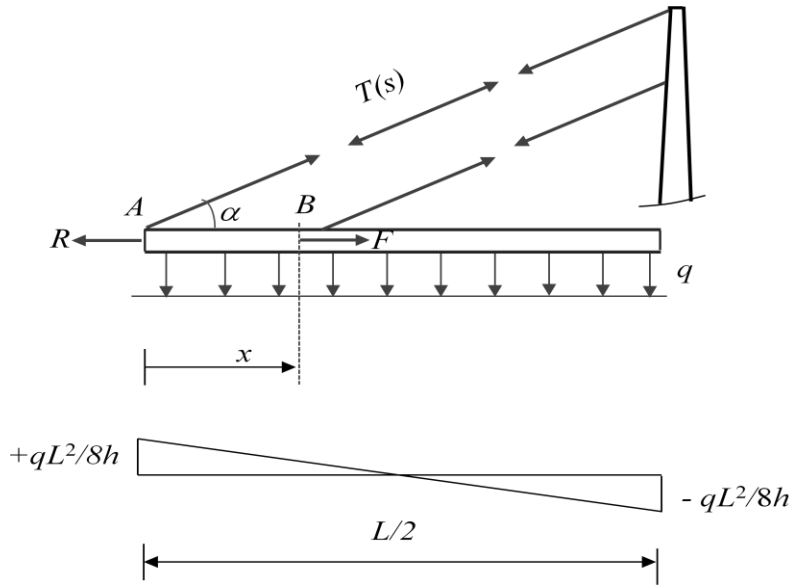


Fig. 2(b). Diagrammatic representation of forces in the uniformly loaded deck developing tension and compression

Assuming that AB (Fig. 2(b)) of length x is acted upon by loads R and F (assumed tensile), then from equation of equilibrium, we have

$$R - \int_0^x T_d dx \sin \alpha \cos \alpha = F \quad (3.3.1)$$

i.e.,

$$R - T_d \sin \alpha \cos \alpha x = F \quad (3.3.2)$$

Substituting $T_d = \frac{q}{\sin^2 \alpha}$ from (3.2.8) gives

$$R - \frac{qx}{\tan \alpha} = F \quad (3.3.3)$$

For a deck of uniform cross-section A and Young's modulus, E , the energy stored in span is

$$U = \int_0^{L/2} \frac{F^2 dx}{2AE} = \frac{1}{2AE} \int_0^{L/2} \left[R - \frac{qx}{\tan \alpha} \right]^2 dx \quad (3.3.4)$$

The energy stored must be a minimum (consistent with the constraints), and so, assuming a rigid attachment at the end, gives

$$\frac{dU}{dR} = 0 = \frac{1}{2AE} \int_0^{L/2} 2 \left[R - \frac{qx}{\tan\alpha} \right] dx = \frac{1}{AE} \left[R \frac{L}{2} - \frac{qL^2}{4} \right] \quad (3.3.5)$$

from which

$$R = \frac{qL}{4\tan\alpha} = \frac{qL}{4\left(\frac{h}{L/2}\right)} = \frac{qL^2}{8h} \quad (3.3.6)$$

and

$$F = R - \frac{qx}{\tan\alpha} = \frac{qL^2}{8h} - \frac{qLx}{2h} = \frac{qL^2}{8h} \left(1 - \frac{4x}{L} \right) \quad (3.3.7)$$

At $x=L/2$, $F = -\frac{qL^2}{8h}$ which means that the outer part of the half-span is in compression, and the middle part, in tension. The change from tensile to compressive force over half-span, is shown in Fig. 2 (b).

The presence of the membrane forces requires an additional volume of deck material, $V_{d,stay}$ given as

$$V_{d,stay} = \frac{qL^2}{8h} \frac{L}{4} \left(\frac{1}{\sigma_{d,t}} + \frac{1}{\sigma_{d,c}} \right), \quad (3.3.8)$$

where $\sigma_{d,t}$ and $\sigma_{d,c}$ are the allowable tensile and compressive stresses in the deck, respectively. Assuming the deck is made of the same material as the pylon, its allowable compressive stress is $\sigma_{d,c} = \sigma_c$, with $\sigma_c = \sigma_t/\gamma$, as used previously. It is assumed further that the allowable compressive stress in the deck is 60% of the tensile one and hence $\sigma_c = 0.6\sigma_{d,t}$, or $\sigma_{d,t} = \sigma_c / 0.6 = (\sigma_t/0.6\gamma)$ and, therefore,

$$\begin{aligned} V_{d,stay} &= \frac{qhL}{32} \left(\frac{L^2}{h^2} \left(\frac{0.6\gamma}{\sigma_t} + \frac{\gamma}{\sigma_t} \right) \right) = \frac{qhL}{32} \left(\frac{L^2}{h^2} \frac{1.6\gamma}{\sigma_t} \right) = \\ &= \frac{qhL}{\sigma_t} \left(\frac{L^2}{h^2} \frac{1.6\gamma}{32} \right) = \frac{qhL}{\sigma_t} (V_{d,stay}^{non-dim}) = \frac{qL^2}{\sigma_t r} (V_{d,stay}^{non-dim}) \end{aligned} \quad (3.3.9)$$

To enable a comparison between the two types of bridges, the deck weight, q , which includes dead and live load, has to be the same in each case. Therefore, the increase in deck weight in this case has to come at the expense of the live load. Thus, for the same design load, q , the cable stay bridge would have to carry a lower live load component of q .

3.4 Volume of material used by the pylons

With reference to Fig. 2(a), if $F(z)$ is the compressive force in the pylon at z , then within the cross section, $A_{pyl}(z)$, the vertical equilibrium gives

$$-\left(F(z) + \frac{dF(z)}{dz} dz\right) + F(z) - (q + \rho_{cbl} g t z) \frac{1}{\sin^2 \alpha} dz - \rho_{pyl} g A_{pyl}(z) dz = 0,$$

which leads to

$$\frac{dF(z)}{dz} = -(q + \rho_{cbl} g t z) \frac{1}{\sin^2 \alpha} - \rho_{pyl} g A_{pyl}(z). \quad (3.4.1)$$

Since $F(z) = \sigma_c A_{pyl}(z)$,

$$\frac{dA_{pyl}(z)}{dz} + \frac{\rho_{pyl} g}{\sigma_c} A_{pyl}(z) = -\frac{1}{\sigma_c} (q + \rho_{cbl} g t z) \frac{1}{\sin^2 \alpha}, \quad (3.4.2)$$

or,

$$\frac{dA_{pyl}(z)}{dz} + \lambda A_{pyl}(z) = -\frac{1}{\sigma_c} (q + \rho_{cbl} g t z) \frac{1}{\sin^2 \alpha}, \quad (3.4.3)$$

where $\lambda = \frac{\rho_{pyl} g}{\sigma_c}$.

Solving for $A_{pyl}(z)$ gives

$$A_{pyl}(z) = C e^{-\lambda z} - \left[\frac{\rho_{cbl} g t}{\sigma_c \lambda^2} (\lambda z - 1) + \frac{q}{\sigma_c \lambda} \right] \frac{1}{\sin^2 \alpha}, \quad (3.4.4)$$

where the constant C is found from the condition that at $z = h$, the cross-sectional area of the pylon vanishes to zero.

Hence

$$C = \frac{q}{\sigma_c \lambda \sin^2 \alpha} e^{\lambda h} + \frac{\rho_{cbl} g t}{\sigma_c \lambda^2 \sin^2 \alpha} e^{\lambda h} (\lambda h - 1)$$

and the cross section area of the pylon is,

$$A_{pyl}(z) = \frac{q}{\sigma_c \lambda \sin^2 \alpha} (e^{\lambda(h-z)} - 1) + \frac{\rho_{cbl} g t}{\sigma_c \lambda^2 \sin^2 \alpha} [(\lambda h - 1) e^{\lambda(h-z)} - (\lambda z - 1)]. \quad (3.4.5)$$

Thus, the volume of the material required by the pylon is

$$V_{pyl,stay} = \int_0^h A_{pyl}(z) dz = \frac{q}{\sigma_c \lambda^2 \sin^2 \alpha} (e^{\lambda h} - 1 - \lambda h) + \frac{\rho_{cbl} g t}{\sigma_c \lambda^3 \sin^2 \alpha} \left[(\lambda h - 1) e^{\lambda h} + 1 - \frac{\lambda^2 h^2}{2} \right] \quad (3.4.6)$$

Expanding to third order,

$$\begin{aligned}
V_{pyl,stay} &= \int_0^h A_{pyl}(z) dz \\
&\approx \frac{q}{\sigma_c \lambda^2 \sin \alpha} \left(\frac{\lambda^2 h^2}{2} + \frac{\lambda^3 h^3}{6} \right) + \frac{\rho_{cbl} g t}{\sigma_c \lambda^3 \sin \alpha} \left(\frac{\lambda^3 h^3}{3} \right)
\end{aligned} \tag{3.4.7}$$

Further manipulations of eqn (3.4.7) and substitutions, involving $t = \frac{q}{\sigma_t} t^{non-dim}$, and $\sigma_c = \frac{1}{\gamma} \sigma_t$ give

$$\begin{aligned}
V_{pyl,stay} &= \frac{q}{\sigma_c \sin \alpha} \left(\frac{h^2}{2} + \frac{\lambda h^3}{6} \right) + \frac{\rho_{cbl} g t}{\sigma_c \sin \alpha} \left(\frac{h^3}{3} \right) \\
&= \frac{q}{\sigma_c \sin \alpha} \left(\frac{h^2}{2} + \frac{\lambda h^3}{6} + \rho_{cbl} g t \frac{h^3}{3} \right) = \frac{q}{\sigma_c \sin \alpha} \left(\frac{h^2}{2} + \frac{\lambda h^3}{6} + \frac{\rho_{cbl} g t^{non-dim} h^3}{\sigma_t} \frac{h^3}{3} \right) \\
&= \frac{q h^2 \gamma}{\sigma_t \sin \alpha} \left\{ \frac{1}{2} + \frac{\lambda h}{6} + \frac{\rho_{cbl} g t^{non-dim} h}{3 \sigma_t} \right\} \\
&= \frac{q h L}{\sigma_t} \left\{ \frac{\gamma h}{L \sin \alpha} \left(\frac{1}{2} + \frac{\lambda}{6} h + \frac{\rho_{cbl} g t^{non-dim} h}{3 \sigma_t} \right) \right\} = \frac{q h L}{\sigma_t} \{ V_{pyl,stay}^{non-dim} \} = \frac{q L^2}{\sigma_t} \frac{1}{r} \{ V_{pyl,stay}^{non-dim} \}
\end{aligned} \tag{3.4.8}$$

The final volume of the material for the supporting elements in a cable-stayed bridge, including self weight of the cables and pylons, and the additional volume of the deck material required to take the membrane forces, is

$$\begin{aligned}
V_{stay}^{total} &= V_{cbl,stay} + V_{d,stay} + V_{pyl,stay} = \frac{q h L}{\sigma_t} \left\{ \frac{1}{2} t^{non-dim} + V_{d,stay}^{non-dim} + V_{pyl,stay}^{non-dim} \right\} \\
&= \frac{q L^2}{\sigma_t} \frac{1}{r} \left\{ \frac{1}{2} t^{non-dim} + V_{d,stay}^{non-dim} + V_{pyl,stay}^{non-dim} \right\}
\end{aligned} \tag{3.4.9}$$

4. Restrictions on spans of suspension and cable-stayed bridges

4.1 Suspension bridges

From eqn (2.3.9), we have

$$\left\{ a - \rho_{cbl} g \frac{L_{cbl}}{\sigma_t} \sqrt{b} \right\} > 0.$$

Since a and b relate to the geometry of the bridge and L_{cbl} to the span, the above restriction imposes a limit on either the span, L , for a given h , or vice-versa.

Let's consider the effect of the span/dip ratio, r , on L . Following the data given in [2] and [8], the allowable tensile strength of cable, σ_t , is taken as 700MPa, and the density of the cable, $\rho_{cbl} g$, equal to 80kN/m³.

Since $a=4h/L=4/r$, $b=1+(4h/L)^2=1+(4/r)^2$, and $\frac{\rho_{cbl} g}{\sigma_t} = \lambda_c$, then introducing $\varphi =4/r$, it can be shown that the limiting span is

$$L = \frac{4\varphi^2}{\lambda_c \left[\ln(\varphi + \sqrt{1 + \varphi^2}) + \varphi\sqrt{1 + \varphi^2} \right] \sqrt{b}}. \quad (4.1.1)$$

Figure 3 and Table 1 illustrate the above relationship, giving maximum limits on span imposed by the weight of the cable. (Shaded area in Table 1 corresponds to the range of r used in practice).

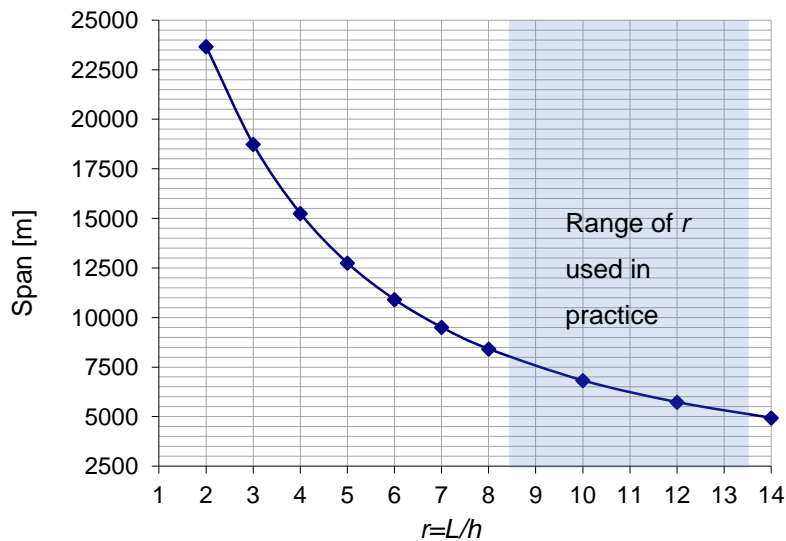


Fig. 3. Suspension cable bridges. Limits on span imposed by cable weight. (Table 1)

$R=L/h$	L [m]
2	23666
3	18737
4	15247
5	12748
6	10906
7	9505
8	8411
10	6822
12	5729
14	4934

Table 1. Suspension cable bridges. Limits on span imposed by cable weight

For the span/dip ratio $r=14$, the limit on span calculated by the current method is 4934 m (just under 5000 m). This finding puts into question the feasibility of building super-long suspension bridges of, say, 5000 m span. As the results indicate, at this span, the relationship (2.3.9) breaks down, as the stress associated with the self weight of cable exceeds the allowable tensile stress, σ_t . Selecting a lower value of r , say $r=10$, would require the height of pylons above the deck to reach 500 m; a value approximately 50% higher than the tallest pylons built in the world to date. This is illustrated by the data shown in Tables 2 and 3.

Bridge name	Main span	Approx. Span/dip	Max. Overall pylon height	Location	Completion date
Akashi Kaikyo	1991 m	9.2	282.8 m	Kobe Awaji route, Japan	1998
Xihoumen	1650 m	10.5	211 m	Zhoushan Archipelago, China	2008
Great Belt (Storebælt)	1624 m	8.8	254 m	Halsskov-Sprogø, Denmark	1998
Runyang South	1490 m	9.6	215 m	Yangtze river, China	2005
Humber	1410 m	11.2	155 m	Hull, UK	1981

Table 2. A selection of largest (completed) suspension cable bridges around the world

Bridge name	Main span	Approx. Span/dip	Max. Overall pylon height	Location	Completion date
Jiangsu Sutong	1088 m	4.5	306 m	Suzhou, Nantong, China	2008
Stonecutters	1018 m	4.5	298 m	Rambler Channel, Hong Kong	2009
Tatara	890 m	4.5	220 m	Seto Inland Sea, Japan	1999
Pont de Normandie	856 m	4	215 m	Le Havre, France	1995
Millau Viaduct	342 m	5	343 m	River Tarn, France	2004

Table 3. A selection of largest (completed) cable-stayed bridges around the world

Apart from a significant increase in aeroelastic problems reported in [9], such a project would require a cable of lower density, possibly varying cross-section area to reduce weight, and/or higher strength than available at present.

4.2 Cable-stayed bridges

From eqn. (3.2.9), we have

$$\sigma_t \sin^2 \alpha - \rho_{cbl} gh > 0$$

Again, this is a unique result, obtained from the refined mathematical model, which includes the contribution of cable weight to the stress field. This contribution must not exceed the allowable stress σ_t .

Using the same material properties as in the previous calculation (section 4.1), and given that $\sin^2 \alpha = 1/(1 + \frac{r^2}{4})$, where $r=L/h$, equation (3.2.9) can be used to calculate the limit for L . This gives

$$L = \frac{r}{\lambda_c \left(1 + \frac{r^2}{4}\right)} \quad (4.2.1)$$

The results illustrating the above relationship are given in Fig. 4 and Table 4. (Shaded area in Table 4 corresponds to the range of r used in practice).

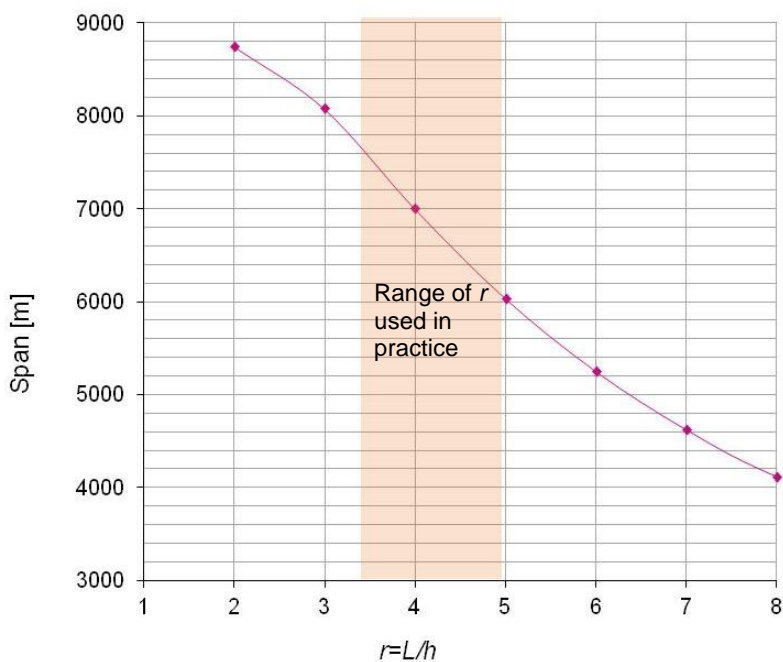


Fig. 4. Cable-stayed bridges. Limits on span imposed by cable weight. (Table 4)

$R=L/h$	L [m]
2	8750
3	8087
4	7000
5	6034
6	5250
7	4623
8	4118
10	3365
12	2838
14	2450

Table 4. Cable-stayed bridges. Limits on span imposed by cable weight

Gimsing² discusses efficiency ratio of a stay cable and builds a model which predicts limits on the span of catenary and suspension cables, due to the cable weight alone. The cables are assumed to

follow a catenary shape that becomes horizontal at the centre span. The results produced by this model should not be interpreted as being applicable to cable-stayed and suspension bridges, because, in the model, the cross section area of cables is calculated from self weight of the cable alone. In bridge applications, the cables are stretched by the applied deck loading and their self-weight. Furthermore, in a cable-stayed structure, the weight of cables is not concentrated in a single catenary, but distributed in a number of cables, none of which adopts a horizontal line at the deck level. In view of this, it is not appropriate to compare results quoted in [2] with the ones presented here (sections 4.1 and 4.2), which are relevant to the actual bridge types.

5. Examples

The mathematical model derived in this paper provides a tool for the analysis of material usage by each type of bridge over a range of span/dip ratios, and for a selection of spans.

In all computational examples, the tensile strength of cable is taken as 1770MPa, and densities of the cable, deck, and the pylons as 80kN/m^3 . The recommended factor of safety⁸ that complies with the Eurocode recommendation is 2.55, and this factor is to be 50% greater than that for structural steel. This gives the allowable tensile strength of cable,

$\sigma_t = 700\text{MPa}$. With the factor of safety for structural steel equal to 1.7 (50% less than that for the cable), the allowable tensile strength of structural steel is assumed to be $460/1.7 = 270\text{ MPa}$. The allowable compressive stress in the deck and pylons is assumed to be 60% lower, giving $\sigma_c = 160\text{ MPa}$. Thus, the ratio of the allowable tensile stress in the cable to the compressive stress in structural steel is $\gamma = 700/160 = 4.375$.

5.1 Suspension bridge

Figure 5 and Table 5 show the material volumes for a 1000 m span, predicted by eqns. (2.2.68), (2.3.8), and (2.4.12) - (2.4.14). It can be seen that the structure reaches an overall minimum, in terms of material usage, for the span/dip ratio, r , equal to 5. The range of r used in practice lies outside this ratio. For all practical values of r , the cable volume constitutes the largest component of the overall volume of material required by the supporting elements.

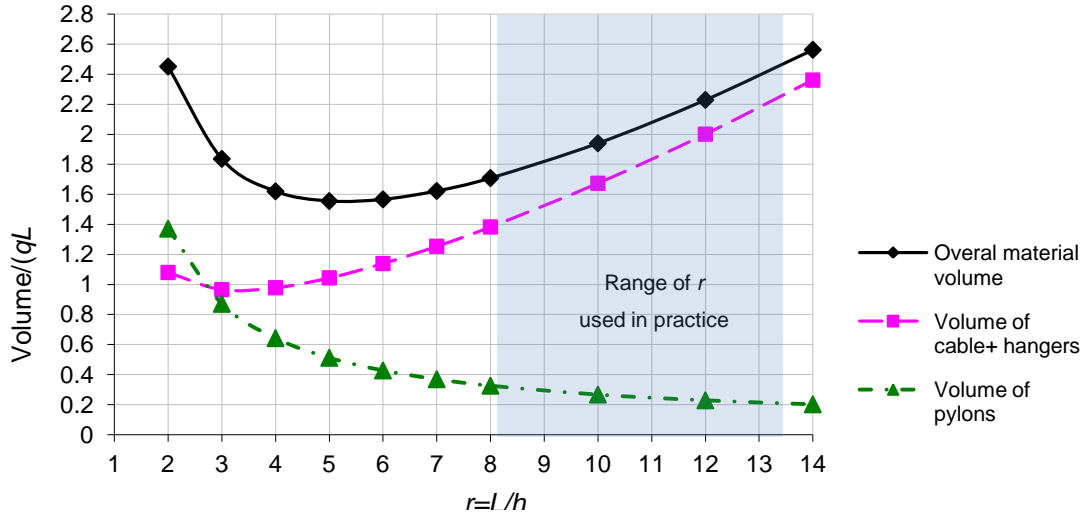


Fig. 5. Suspension bridge of 1000 m span. Material volumes. (Table 5)

Recognising the fact that, in practice, the unit cost of cable is higher than that of pylon, Figure 6 presents the results for cases of $C_{cbl}/C_{pyl}=1, 1.5,$ and 2.0 respectively, where C_{cbl} is the unit cost of cable+hanger, and C_{pyl} that of pylon. The results for a 1000 m span show that the increases of cable+hanger unit costs by 50%, and 100% , relative to those of structural steel (pylons) have not altered the value of the optimum span/dip ratio, r , which remains as 5. They also show that for cases of $C_{cbl}/C_{pyl}=1.5$ and 2.0 , with $r=10$, there is an increase of 30%-40% in the cost of material used by the supporting elements, compared to the optimum $r=5$. This increase reaches 50%- 60% for the case of $r=12$.

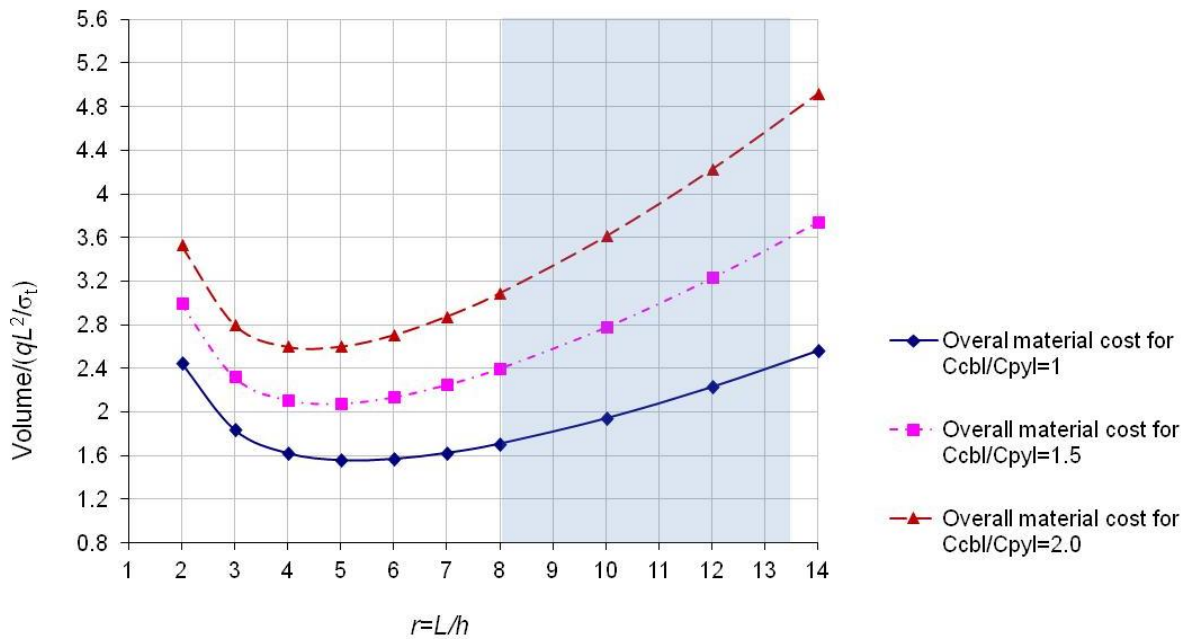


Fig. 6. Suspension bridge of 1000 m span. The effect of unit cost of cable relative to that of structural steel (pylon) on overall material costs

Figure 7 examines the effect of bridge size on material requirements, by using spans varying between 500 m and 3000 m. It can be seen that the minimum usage of the material corresponds, again, to $r = 5$. For spans of 500 m and 1000, there is a modest increase in the volume of the material over the range of r used in practice. The increases in the volume of the material for spans 2000 m (and higher), become significant for $r = 10 - 12$. These increases are: approximately 30% - 60%, for span of 2000 m, and 40%-100% for span of 3000 m.

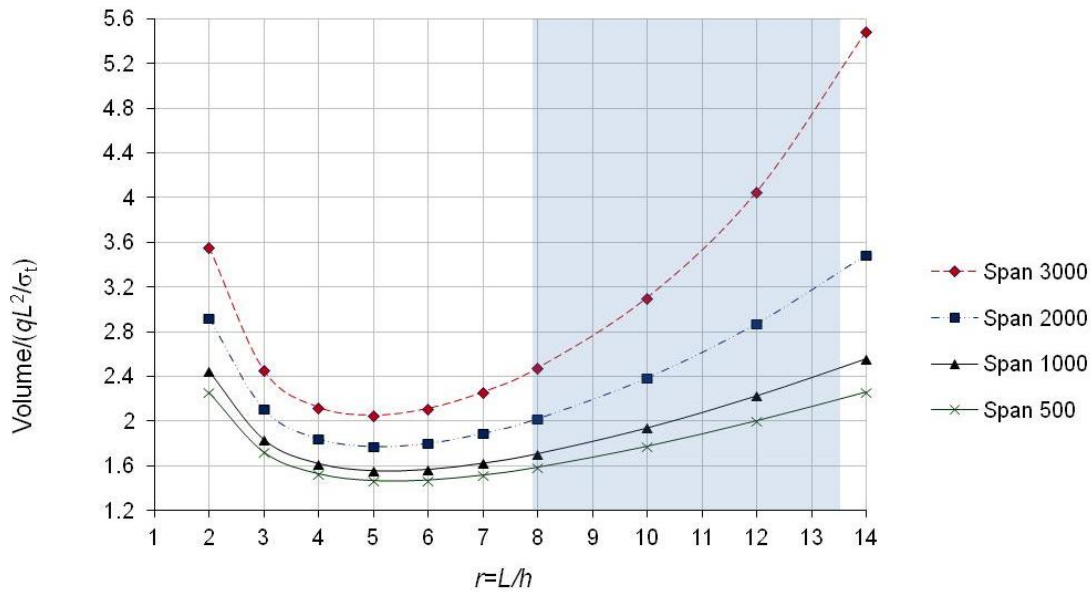


Fig. 7. Suspension bridge. Effect of span size on the overall volume of material

The observations presented above relate to the costs of materials of supporting elements only, not the overall costs that would normally include construction.

5.2 Cable-stayed bridge

Figure 8 and Table 5 show the material volumes for a 1000 m span, given by eqns. (3.2.12), (3.3.9), (3.4.8)= (3.4.9).

The results show that the structure reaches an overall minimum, in terms of material usage, for the span/dip ratio, r , equal to 3. Again, the range of r used in practice lies just outside this ratio. For values of r between 4 and 5, and the stress pattern considered in Fig. 2(b), the additional deck weight accounts for a significant overall volume of the supporting elements, and a similar observation can be made with regard to the cable volume. In order to carry out meaningful comparisons with the suspension bridge, the increase in deck weight in the cable-stayed bridge has to come at the expense of the live load component of q .

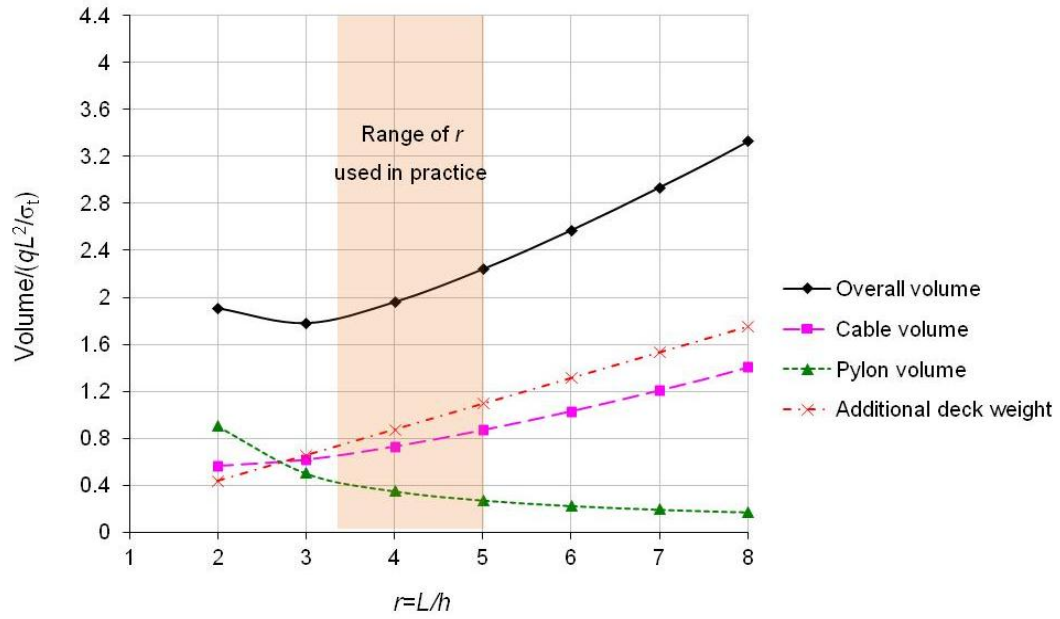


Fig. 8. Cable-stayed bridge of 1000 m span. Material volumes. (Table 5)

$r=L/h$	Suspension structure				Cable - stayed structure			
	$1/r * V^{non-dim}$				$1/r * V^{non-dim}$			
	Hangers	Cable	Pylons	Total	Cables	Deck weight	Pylons	Total
2	0.1667	0.9130	1.3714	2.4511	0.5645	0.4375	0.9044	1.9064
3	0.1111	0.8543	0.8708	1.8362	0.6182	0.6562	0.5038	1.7782
4	0.0833	0.8946	0.6420	1.6199	0.7292	0.8750	0.3524	1.9566
5	0.0667	0.9772	0.5115	1.5554	0.8690	1.0938	0.2746	2.2374
6	0.0556	1.0837	0.4273	1.5666	1.0294	1.3125	0.2276	2.5695
7	0.0476	1.2064	0.3686	1.6226	1.2077	1.5312	0.1963	2.9352
8	0.0417	1.3413	0.3254	1.7084	1.4033	1.7500	0.1740	3.3273
10	0.0333	1.6403	0.2663	1.9399	1.8496	2.1875	0.1448	4.1819
12	0.0278	1.9730	0.2281	2.2289	2.3805	2.6250	0.1272	5.1327
14	0.0238	2.3372	0.2016	2.5626	3.0172	3.0625	0.1162	6.1959

Table 5. Comparison of material volumes for 1000 m span: suspension bridge versus cable-stayed

In assessing material costs, values of C_{cbl}/C_{pyl} of 1, 1.5, and 2.0 are used, as in the case of the suspension bridge. The results of the analysis for the 1000 m span are shown in Figure 9.

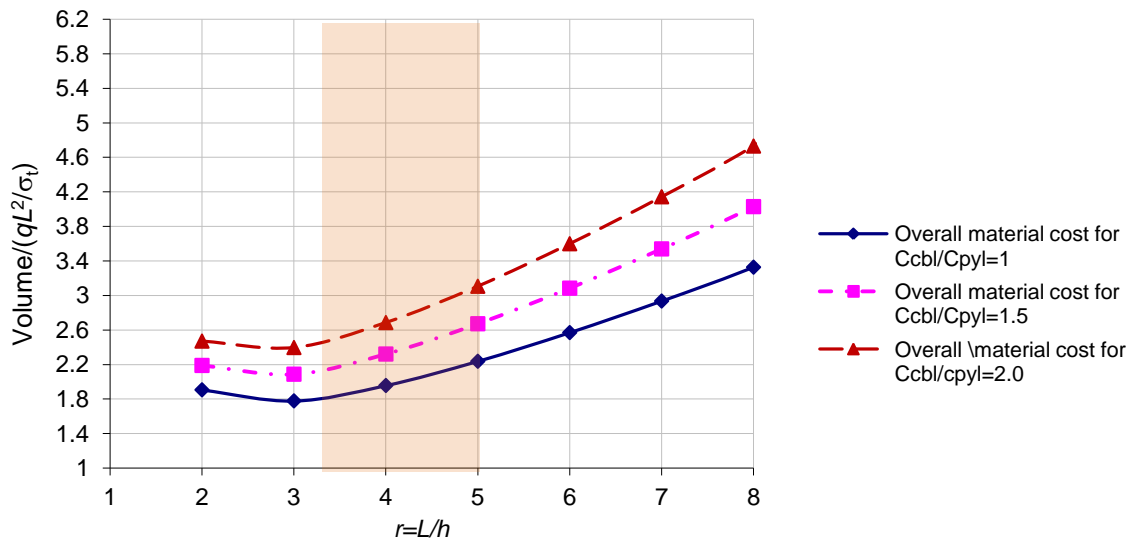


Fig. 9. Cable-stayed bridge of 1000 m span. The effect of unit cost of cable relative to that of structural steel (pylon) on overall material costs

It can be seen that the increases of cable unit costs by 50%, and 100% , relative to those of structural steel have not altered the value of the optimum span/dip ratio, which remains as 3. For the case of C_{cbl}/C_{pyl} equal to 1.5 and 2.0, with $r=5$, there is an approximately 30%-40% increase in the cost of material used by the supporting elements, compared to the optimum value of r equal to 3.

The effect of size of the bridge on the material requirements is examined in Fig. 10. The results show that the minimum usage of the material corresponds to, again, $r = 3$. When the span increases from 500 m to 1000 m, there are modest increases in the volume of the material, over the range of r used in practice. These increases become significant for larger spans, e.g., approximately 35% for the span of 2000 m.

Again, the above observations relate to the costs of materials of supporting elements only, not the overall costs that would normally include construction.

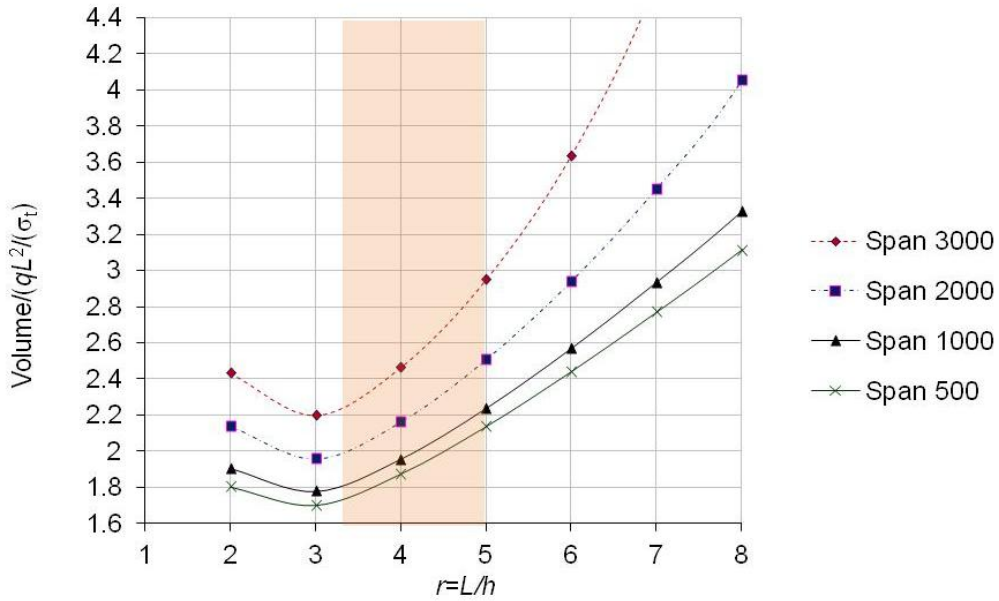


Fig. 10 . Cable-stayed bridge. Effect of span size on the overall volume of material

5.3 Suspension bridge versus cable-stayed

A comparison of material volumes for the supporting elements in the two types of bridges, both of 1000 m span, is given in Fig. 11.

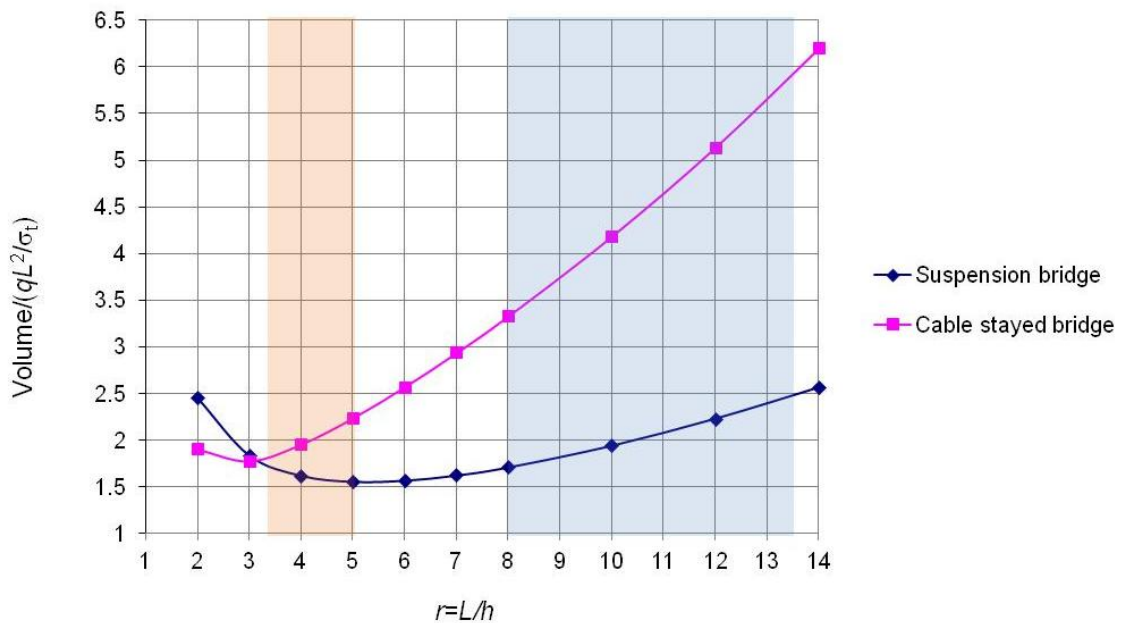


Fig. 11. Comparison of material volumes for a 1000 m span: suspension bridge versus cable-stayed

It can be seen that for the relevant ranges of r used in practice, i.e., 3.5-5 for the cable stayed bridges, and 8-12, for the suspension bridges, the latter require less material. When comparing the results for optimum ratios: $r = 5$ (in the case of the suspension bridge), and $r = 3$ (for the cable- stayed), they show that a suspension bridge requires approximately 14% less material. A comparison of the material costs is given in Figure 12.

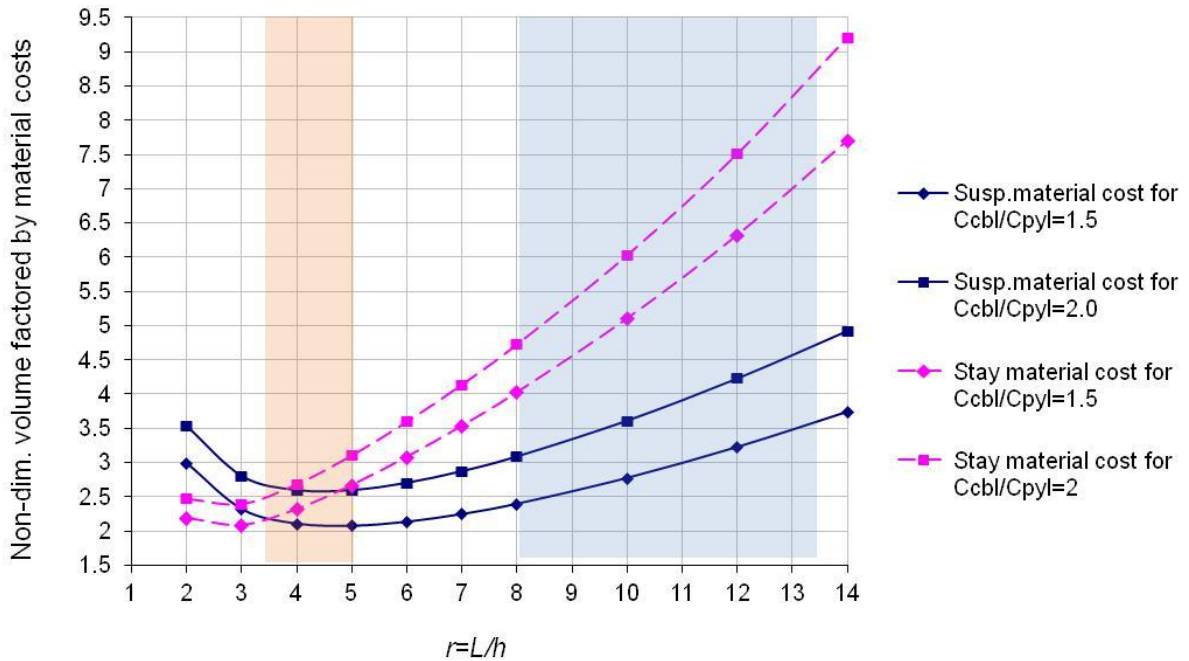


Fig. 12. Comparison of material costs for a 1000 m span: suspension bridge versus cable-stayed.

Considering the common range of span/dip ratios used in practice, it can be seen that suspension bridges with $r = 8-10$ are marginally less expensive than the cable stayed ones with $r = 5$, but become 30% , or more, expensive for $r = 12$ and above. Interestingly, when comparing the results for the optimum span/dip ratios, i.e., $r = 3$ for the cable-stayed bridge, and $r = 5$ for the suspension structure, the two appear to have similar material costs for $C_{cbl}/C_{pyl} = 1.5$, but the suspension bridge becomes more expensive when $C_{cbl}/C_{pyl} = 2.0$.

In the above comparisons, it is important to note again that for the same design load q , the dead weight component is greater in the cable-stayed bridge, due to the additional weight of decking. This leaves the live load component reduced by the equivalent amount. In view of this, the suspension bridge is a more material efficient structure.

6. Summary and Conclusions

The paper presents a refined mathematical model for the relative assessment of material requirements by the supporting elements in suspension and cable-stayed bridges. It is assumed that each structure is made of the same material (steel) and carries an identical design load, q , exerted by the deck. Cables are assumed to be of constant cross-section. In the case of the suspension bridge, they follow a parabolic shape, and, in the case of the cable-stayed structure, straight lines (approximation to shallow catenaries). Calculations are confined to a centre span of a three-span bridge, with the size of the span ranging from 500 m to 3000 m. The cross-section of pylons is such as to maintain constant stress.

Results show that the optimum span/dip ratio, which minimises material usage, is 3 for a cable-stayed (harp type) bridge, and 5 for a suspension structure. These values fall into the range quoted by Croll⁷, but lie outside the ranges of span/dip ratios used in practice where construction costs and practical limits on the pylon height are considered. With regard to the latter, data given in Tables 2 and 34, concerning the largest suspension¹⁰ and cable-stayed bridges¹¹ in the world, shows that the highest pylons built to date are for the Millau Viaduct (343 m overall). This record may be broken by the proposed Strait of Messina suspension bridge¹² with a 3,300 m main span, the overall height of pylons of 382.6 m, and a span/dip ratio $r = 10.4$.

The inclusion of the self weight of cable in the analyses produced quantifiable limits on spans of the two types of structures at which the stresses generated by cable weight alone could exceed the limit on the allowable tensile strength of the cable. In the case of the suspension bridge, this limit is just less than 5000 m. This result raises a question over the feasibility of super-long bridges of 5000 m planned for the future⁹ with currently available material densities and strengths of cable.

A comparison of material costs of the supporting elements in the suspension and cable-stayed bridges revealed that, for the range of span/dip ratios used in practice, the two costs are similar when the unit cost of cable is 50% higher than that of the pylons, but the suspension bridge becomes more expensive when this cost is doubled.

It should be noted that, for the same design load q , the dead weight component of q is greater in the cable-stayed bridge, due to the additional weight of decking necessary to take the membrane forces. This automatically lowers the live load component of q for the cable-stayed bridge. In view of this, it can be concluded that the suspension bridge is a more material efficient structure.

The overall results highlight the importance of the span/dip ratio in regulating the volume and cost of the material required. In the case of the suspension bridge of 1000 m main span, they show that for cases of $C_{cbl}/C_{pyl}=1.5$ and 2.0, with $r=10$, there is an increase of 30%-40% in the cost of material used by the supporting elements, when compared with the results for the optimum $r=5$. This increase reaches 50%-60% for the case of $r=12$. A similar analysis for the 2000 m span gives increases between 40%-60% and 70%-90%, respectively. In the case of a cable-stayed bridge, a comparison of material costs for the optimum $r=3$, and results obtained for $r=5$ show similar increases (30%-40%) for the span of 1000 m.

Larger spans lead to a high span/dip ratio, because of practical limits of pylon heights. This, increases material requirements and, consequently, raises sustainability issues and concerns over environmental costs.

7. References

1. French, M, *Conceptual Design for Engineers*, Springer, 3rd Ed, 1999, pp.58-59.
2. N. S, Gimsing, "Cable Supported Bridges". John Wiley & Sons, 1998.
3. W. Podolny and J.B. Scalzi, "Construction and Design of Cable-Stayed Bridges". John Wiley & Sons, 1976, pp. 60-61.
4. F. Leonhardt and W. Zellner, "Vergleiche zwischen Hängebrücken und Schrägkabel-brücken für Spannweiten über 600 m. International Association for Bridge and Structural Engineering, vol. 32, 1972.
5. M.F. Parsons, "Engineering Structures. Developments in the Twentieth Century: a Collection of Essays to Mark the Eightieth Birthday of Sir Alfred Pugsley", edited by Bulson, P.S., Cadwell, J.B. and Severn, R.T.. Chapter 4 - Suspension Bridges. University of Bristol Press, 1983.
6. J. G. A. Croll, "Structural Efficiency of Cable-stayed and Catenary Suspension Bridges". *The Structural Engineer*, Vol. 75, No. 10, 1997, pp. 173-175.
7. H.C. Dalton, M.J. French and J. G. A. Croll, "Thoughts on the Structural Efficiency of Cable-Stayed and Catenary Suspension Bridges". *The Structural Engineer, Correspondence*, Vol. 75, No. 19, 1997, pp. 345-347.
8. Flint & Neill Partnership/Ammann&Whitney, "Audit of the main Cable Inspection and Assessment: Final Report" APPENDIX C. Scottish Government publications.
<http://www.scotland.gov.uk/Publications/2006/03/03154220/19>.

9. Ge Yao-Jun and Xiang Hai-Fan, “ Aerodynamic Challenges in Long-span Bridges, Proc. IStructE Centenary Conference, Hong Kong, 2008. The Institution of Structural Engineers, 2008, pp. 120-143.
10. http://en.wikipedia.org/wiki/list_of_longest_suspension_bridge_spans.
11. http://en.wikipedia.org/wiki/list_of_largest_cable-stayed_bridges.
12. http://en.wikipedia.org/wiki/Strait_of_Messina_Bridge.

List of Figures

- Fig .1. Basic geometry of a suspension cable bridge
- Fig. 1(a). Diagrammatic representation of forces in the main structural elements of the bridge
- Fig. 2. Basic geometry of a cable-stayed bridge
- Fig. 2(a). Diagrammatic representation of forces in the main cable and the pylon
- Fig. 2(b). Diagrammatic representation of forces in the uniformly loaded deck developing tension and compression
- Fig. 3. Suspension cable bridges. Limits on span imposed by cable weight. (Table 1)
- Fig. 4. Cable-stayed bridges. Limits on span imposed by cable weight. (Table 4)
- Fig. 5. Suspension bridge of 1000 m span. Material volumes. (Table 5)
- Fig. 6. Suspension bridge of 1000 m span. The effect of unit cost of cable relative to that of structural steel (pylon) on overall material costs
- Fig. 7. Suspension bridge. Effect of span size on the overall volume of material
- Fig. 8. Cable-stayed bridge of 1000 m span. Material volumes. (Table 5)
- Fig. 9. Cable-stayed bridge of 1000 m span. The effect of unit cost of cable relative to that of structural steel (pylon) on overall material costs
- Fig. 10 . Cable-stayed bridge. Effect of span size on the overall volume of material
- Fig. 11. Comparison of material volumes for a 1000 m span: suspension bridge versus cable-stayed
- Fig. 12. Comparison of material costs for a 1000 m span: suspension bridge versus cable-stayed.

List of Tables

- Table 1. Suspension cable bridges. Limits on span imposed by cable weight
- Table 2. A selection of largest (completed) suspension cable bridges around the world
- Table 3. A selection of largest (completed) cable-stayed bridges around the world
- Table 4. Cable-stayed bridges. Limits on span imposed by cable weight
- Table 5. Comparison of material volumes for 1000 m span: suspension bridge versus cable-stayed